Naval Research Laboratory
Washington, DC 20375-5320

NRL/MR/6755--99-8313

Radar Studies of the Solar Corona: A Review of Experiments Using HF Wavelengths

PAUL RODRIGUEZ

Charged Particle Physics Branch
Plasma Physics Division

Invited Paper
Chapman Conference on Space Based Radio Observations at Long Wavelengths
October 19-23, 1998
Paris, France

January 29, 1999

REPORT DOCUMENTATION PAGE

Form Approved
OMB No. 0704-0188

1. AGENCY USE ONLY (*Leave Blank*)	2. REPORT DATE	3. REPORT TYPE AND DATES COVERED
	January 29, 1999	Interim

4. TITLE AND SUBTITLE

Radar Studies of the Solar Corona: A Review of Experiments Using HF Wavelengths

5. FUNDING NUMBERS

6. AUTHOR(S)

Paul Rodriguez

7. PERFORMING ORGANIZATION NAME(S) AND ADDRESS(ES)

Naval Research Laboratory
Washington, DC 20375-5320

8. PERFORMING ORGANIZATION REPORT NUMBER

NRL/MR/6755--99-8313

9. SPONSORING/MONITORING AGENCY NAME(S) AND ADDRESS(ES)

10. SPONSORING/MONITORING AGENCY REPORT NUMBER

11. SUPPLEMENTARY NOTES

12a. DISTRIBUTION/AVAILABILITY STATEMENT

Approved for public release; distribution unlimited.

12b. DISTRIBUTION CODE

13. ABSTRACT (*Maximum 200 words*)

The use of high frequency (9 to 40 MHz), high power radars to study the solar corona has a remarkable history. Solar radar experiments were proposed and started at the beginning of the modern era of space physics research. Early in the 1960's the El Campo solar radar facility began routine operations. The published results from these pioneering experiments remain our largest resource of information on active probing of the solar corona. In 1969, solar radar experiments ceased even though experimental results suggested that significant diagnostics of the solar corona could be obtained with this technique. After the El Campo facility was decommissioned, a hiatus of about 25 years followed for further solar radar experiments. Recently, high frequency radar facilities in Russia and Ukraine have been used to conduct new solar radar experiments. The information that solar radars may provide is particularly relevant today, as we now recognize the important role of coronal mass ejections in geomagnetic disturbances. Solar radars offer the possibility of direct detection of earthward-moving coronal mass ejections, providing several days of advance warning to possible geomagnetic storms. In addition, investigations of wave scattering in the solar corona may provide information on coronal densities and irregularities. The techniques derived for studies of the earth's ionosphere using incoherent scatter radars are potentially applicable to the solar corona as well. We will review the early and current solar radar experiments and also discuss future directions for radar studies of the solar corona.

14. SUBJECT TERMS

15. NUMBER OF PAGES
26

16. PRICE CODE

17. SECURITY CLASSIFICATION OF REPORT	18. SECURITY CLASSIFICATION OF THIS PAGE	19. SECURITY CLASSIFICATION OF ABSTRACT	20. LIMITATION OF ABSTRACT
UNCLASSIFIED	UNCLASSIFIED	UNCLASSIFIED	UL

NSN 7540-01-280-5500

Standard Form 298 (Rev. 2-89)
Prescribed by ANSI Std 239-18
298-102

Radar Studies of the Solar Corona: A Review of Experiments Using HF Wavelengths

1. Introduction

Studies of the solar corona with high frequency radars were first done in the early 1960s by groups from Stanford University [Eshelman et al., 1960] and the Massachusetts Institute of Technology's (MIT) Lincoln Laboratory [Abel et al., 1961, 1963]. These experiments were begun to test theoretical ideas suggested by Kerr [1952] and by Bass and Braude [1957]. In subsequent years, from 1961 to 1969, the MIT group developed a sustained program of experiments using a radar facility specially designed for the solar studies and constructed in El Campo, Texas. The El Campo solar radar operated as both a transmitting and a receiving array for high frequency (HF) radio waves at 38.25 MHz. The results of the El Campo experiments have been summarized and reviewed by James [1968] and show that return signals were detected that suggested a radar cross section for the sun's corona of approximately the same size as the optical disk, with occasional cross-section enhancements by an order of magnitude or more. Consistently, Doppler shifts in the return signals of about 4 kHz to 15 kHz were detected, and these were attributed to mass motions in the solar corona. Such motions were identified with the outward flow of the solar wind from the base of the corona. Theoretical studies of the results of the El Campo solar radar tests have been published by Gordon [1968, 1969, 1973], Gerasimova [1975, 1979], Wentzel [1981], Owocki et al. [1982], Chashei and Shishov [1994], and Mel'nik [1998]. These studies have suggested that radar return signals can provide important new diagnostic information on the structure and dynamics of the solar corona. Unfortunately, after 1969 further solar radar experiments were not possible because the El Campo solar radar was deactivated and no longer exists.

In the early experimental and theoretical studies, the possibility of detecting coronal mass ejections (CMEs) with solar radars was not specifically identified, probably because it was only later (in the 1970s) that CMEs were recognized as distinct large-scale coronal perturbations. It is possible that in some of the El Campo measurements, the signature of CMEs was recorded but remained unrecognized. The now-known fact that CMEs are capable of causing major geomagnetic storms at earth [monograph edited by Crooker et al., 1997] has motivated new interest in solar radars to detect earthward-moving CMEs [Rodriguez, 1996]. For an earthward-moving CME, it is expected that a return signal might have a distinct Doppler shift associated with the earthward-directed velocity. Based on the known distribution of CME velocities, a wide range of Doppler shifts, up to 100 kHz, would be expected on HF return signals. The large-scale structure of a CME may also mean that the radar cross section would be larger than that of the quiescient corona. The early solar radar investigations also did not have the benefit of modern solar monitoring stations to provide correlative imaging of the corona, such as the the SOHO satellite, the Mauna Loa coronameter, and various national observatories that provide daily reports of solar activity.

Manuscript approved December 9, 1998.

Beginning in the summer of 1996, an international consortium of investigators (see Appendix) has conducted several new solar radar tests using facilities in Russia and Ukraine. The high power HF transmitting array SURA located near Nizhny Novgorod, Russia, has been used in a bistatic configuration with the HF receiving array UTR-2 located near Kharkov, Ukraine, to conduct several experiments. In overall operational characteristics, the SURA/UTR-2 bistatic configuration approximates the El Campo facility except in operating frequency; El Campo used 38.25 MHz, whereas SURA/UTR-2 is presently restricted to a maximum of about 9.3 MHz. The principal motivations of new solar radar experiments have been to begin development of new techniques to identify earthward-moving CMEs and to use these techniques to study the solar corona. A greater understanding of coronal dynamical processes would be important to models of the development of CMEs and their subsequent effects at earth. The potential for providing several days' warning that large geomagnetic storms may occur is an attractive practical benefit. In the following sections of this report, we will discuss experimental results from both El Campo and SURA/UTR-2.

In the years since the El Campo experiments, the study of the earth's ionosphere with HF radars has provided well-established procedures and techniques that may carry over to studies of the solar corona. Such modern diagnostic techniques were not available to the early solar radar investigators. In addition, recent HF radar experiments with the near-earth space plasma have become possible. These experiments include studies of the solar wind [Genkin and Erukhimov, 1990; Genkin et al., 1991] and the magnetosphere [Gurevich et al., 1995]; experiments to detect the earth's magnetopause are also planned. New possibilities for the use of combined HF radars and satellite experiments have also been demonstrated in experiments with the NASA/WIND spacecraft [van't Klooster et al., 1997; Rodriguez et al., 1998].

2. Review of El Campo Observations

The principal results of early solar radar observations can be found in the review by J. C. James [1968], several succeeding papers [James, 1970a; 1970b], and references therein. The fundamental basis of solar radar experiments is that coronal electron densities are typically in the range corresponding to electron plasma frequencies from about 5 to 100 MHz. The radial dependence of the average quiescent coronal electron density is generally an inverse power law for which several models have been derived. The range of plasma frequencies listed above corresponds to coronal radial distances of about 10 R_o to 1 R_o (where R_o is in solar radii) for the electron density models used by James (Pottasch and Baumbach-Allen models), [Pottasch, 1960; Allen, 1973]. An electromagnetic wave at a given frequency propagating into a plasma of increasing electron density encounters an index of refraction decreasing from the free-space value of 1 to 0 when the wave frequency equals the plasma frequency. This decrease of refractive index generally causes a turning in the direction of propagation of the wave and can result in reflection of the wave. Thus, an earth-launched electromagnetic wave entering the corona can be reflected from a coronal height where the wave frequency and the local plasma frequency are equal. However, for a turbulent and structured corona, the wave-reflection mechanism described above is probably too simple; a return signal is expected to be the result of more complex linear and nonlinear wave-plasma interactions. Such

interactions, if properly diagnosed, may provide new information on coronal plasma dynamics. Fortunately, coronal electron densities are mostly greater than electron densities in the earth's ionosphere, so that the required frequencies for a solar radar can pass through the earth's ionosphere both on transmission and return.

In Figure 1, we show a photograph of the El Campo solar radar array. The array was formed from 1024 half-wave dipoles used as both transmitting and receiving antennas. A cross-polarized receive-only array was later added, consisting of 512 dipoles. The facililty operated at a total transmitted power of about 500 kW. At a half-power beamwidth of about 1° north-south by 6° east-west, the antenna gain factor was 32 to 36 dB, resulting in an effective radiated power of about 1300 MW. The array could be phased manually to allow repositioning of the main lobe according to the change of the sun's apparent elevation throughout the year. During a given transit by the sun at local noon, the east-west beamwidth was wide enough to allow 16 minutes of transmission followed by 16 minutes of reception, where 16 minutes is the travel time of electromagnetic waves to the sun and back. The normal mode of operation was to transmit at two frequencies, offset from 38.25 MHz by several tens of kHz. The transmission was switched between the two frequencies according to a pseudo-random code that provided a known ON-OFF sequence of each frequency. The most common pulse widths used were 0.5 to 2 seconds, corresponding to a range resolution of about 0.1 to 0.4 R_o. The received signal was correlated with the known sequence of ON-OFF pulses and integrated in 20 range "boxes." Each range box corresponded to a time delay in the return signal and was associated with a radial distance interval in the solar corona. The recorded signal bandwidth was adjusted for various ranges of frequency shifts in the return signal, up to about 60 kHz, so that the final output consisted of a spectrum of total integrated power in about 20 by 10 range-frequency shift boxes. These spectra of the return signal, referred to as the solar echo spectra, were the basis of analysis and interpretation.

In Figure 2a and 2b, we show a series of data plots extracted from El Campo publications that illustrate the measurements. When examining these measurements, it is important to understand that all of the El Campo results were derived with integration techniques. The return signal is weak and always below the minimum background noise level, which is set by the solar HF background. Only by integration can the signal to noise ratio be made equal to or greater than 1. In Figure 2a, the four data panels show a series of what were probably exploratory measurements taken during the first years of operation in which the pulse width of the transmitted waves was reduced from 8 sec to 1 sec. Reducing the pulse width increased the range resolution and simultaneously reduced the total range covered by the 20 integration boxes. Thus, with 8-sec pulse width, the measurement shows the maximum return power, relative to background, occurring in integration box number 16, whose time delay corresponds to a position centered on about 1.5 R_o. However, because of the long pulse width, there is little resolution of the region of maximum power return. The sequence of data plots as the pulse width is reduced illustrates the general increase of resolution of the region near 1.5 R_o, and the corresponding decrease of total range to about $\pm$ 2 R_o about the sun. The data plots of Figure 2a consist only of the total relative power versus range. In Figure 2b, El Campo data are displayed in spectral format, in which pulse widths of 0.5 sec were used and the frequency shift for each range box is also resolved, in frequency intervals of about 5 kHz. Most of the El Campo data which are

published are in the format shown in Figure 2b. Total relative power in each spectral cell is indicated by the height of darkening. In this figure, the data indicate the strongest signal return occurring from a broad region centered at about 1.2 R_o with frequency shifts from about -5 kHz to about +25 kHz. The interpretation given to such data is that the solar echo comes from a range of coronal longitudes, including the eastern and western sides of the corona. Because the minimum beamwidth used is about 1°, the disk of the sun itself (about 0.5° in angle) cannot be resolved; thus, return power is integrated over a cross field range of about 2 R_o in dimension. Frequency shifts were interpreted as Doppler shifts resulting from moving coronal plasma that becomes the solar wind. During the years of El Campo operations, several categories of spectral plots were derived, which were based on certain recurring characteristics. Among these categories were the "high coronal echoes," corresponding to relative maximum signals located at about 2 R_o. These type spectra showed both "narrow" and "broad" Doppler shifts, suggesting various levels of ordering to coronal plasma motion.

In light of our current understanding of coronal dynamics, it is possible that some of these high coronal echoes may have been associated with coronal mass ejections. Unfortunately, the only correlative observations available at that time seems to have been the sunspot number. The El Campo results show that the radar cross section of the solar corona showed a positive correlation with sunspot number and was taken to indicate that increasing solar activity increased the power of return signals. Various reasonable interpretations for this correlation were given, and some models were suggested, which came close to what might be conceived of as coronal mass ejections, but the phenomenon of CMEs as we know it today (a large scale coronal disturbance) was not considered. Nevertheless, the published El Campo data are impressive, and our contemporary knowledge suggests that similar measurements made today could significantly increase our understanding of the solar corona, especially if these measurements were done in correlation with other coronal observations, such as those of white-light coronagraph images. It is very fortuitous that the same radial range in the corona is covered by coronagraph images and HF radar observations. Thus, the same electron densities that scatter white light for coronagraph images are responsible for the HF solar echo. There are few places in the space environment where such a coincidence of measurement parameters occurs.

3. New Solar Radar Experiments

The possibility that CMEs can be detected with HF solar radars is suggested by the El Campo observations. In order to test this concept, it would be desireable to use radar facilities that are close equivalents to El Campo. Such facilities may be found in some of the high power HF radars that are presently in operation. Among these are ionospheric "heating" facilities, which began to be developed at about the same time as the El Campo facility, although their objective was to study modifications and wave interactions in the earth's ionosphere. These facilities were designed to transmit at frequencies below about 10 MHz, so that the waves would be absorbed and scattered at ionospheric altitudes. In addition to the ionospheric radars, another type of high power radar available was developed for planetary studies. Planetary radars are designed to detect returns from planetary hard surfaces, such as those of Venus and the moon. For these experiments, frequencies in

the several hundred MHz range are needed (for example, the Arecibo radar operates at 435 MHz). These higher frequencies are in fact too high for the solar corona investigation because they propagate far into the corona and reach photospheric heights where absorption dominates and no return signal occurs. The optimum frequency window for solar radar experiments is in the tens of MHz range, so El Campo was designed for 38.25 MHz. As of today, the only high power radars operating in this range are over-the-horizon radars designed by the military for long-range surveillance. These radars, however, have been constructed to form their transmit and receive beams at low elevation angles in specific azimuth directions so that the ionosphere can be used to reflect the waves around the curve of the earth's surface. This configuration is disadvantageous for a solar radar because only sunrise or sunset conditions can be used, and only if sunrise or sunset occurs within the azimuth direction of the main beam.

In our estimation (see Table 1), the best current facility for solar radar experiments is formed from the combination of the Russian SURA ionospheric heating facility and the Ukrainian UTR-2 radio astronomical array. A schematic drawing of the bistatic configuration used and the experiment concept is shown in Figure 3. Photographs of these facilities are included in the Appendix. The drawing of Figure 3 represents an earthward-directed CME, with the return signal coming from the 1 R_o to 5 R_o range. In the lower right corner is a schematic of the frequency spectrum of the solar echo that might occur. The transmitted signal is shown as a single frequency at high power; the return signal is broadened by both random and directed motion in the corona. If a CME is present, it is expected to be a generally large-scale structure moving approximately as a single entity; thus, the power return may be greater and the frequency shift narrower than the background coronal plasma. Such a signature is reminiscent of the high coronal echoes of the El Campo data. In the Appendix, we list characteristics of the SURA and UTR-2 facilities relevant to the solar radar investigation. In addition to the ground-based facilities, we have made extensive use of the NASA/WIND spacecraft to provide a space-based receiver for the SURA-transmitted signals. This use of a ground-based radar in combination with space experiments was not available to the early solar radar experiments and provides the additional advantage of measurements of the influence of the earth's ionosphere on the high power signal launched toward the sun. An understanding and knowledge of possible ionospheric effects are important for subsequent analysis of return signals, especially at the lower frequency we must currently use. The characterisitics of the WAVES experiment onboard WIND are also described in the Appendix.

4. Experiments Conducted

Beginning in the summer of 1996, we have conducted three limited series of experiments with the SURA/UTR-2 bistatic configuration. Initial tests involved transmission at full power with 5- to 10-sec pulses alternating between two frequencies in a periodic waveform. The transmission frequencies were determined by surveys of interference backgrounds observed at both transmit and receive sites. Generally, the two most common frequencies used for transmission from SURA were 8.920 and 8.880 MHz. At the UTR-2 site, reception was done with receivers with about 40 kHz bandwidth. Digital waveform measurements were made of the baseband frequency with 2x40 kHz sampling rate, and the analog signal was also recorded on magnetic tape. Several other types of

received signal measurements were made using high-speed correlometers and total power detectors. On the selected summer days, SURA transmission occurred for the 16-minute interval UT 0911 to 0927, corresponding to near local noon, when the visible sun was within the main lobe of the SURA array. A periodic square wave modulation with pulse period of 20 sec switched the transmission frequency between 8.920 and 8.880 MHz, with ON pulse width of 10 sec. Thus, the full power of 750 kW was ON at all times, either in one frequency or the other. Other pulse periods and widths were also used; however, we discuss only this one mode in this report. Signals were recorded at UTR-2 in three phases: during transmission from SURA (with receiver front end attenuation of 30 dB), during the time interval of the expected return signal (receiver front end attenuation set to 0 dB), and after the return signal time period to obtain background measurements (receiver front end attenuation also at 0 dB). Data obtained during the return signal time interval (UT 0927 to 0943) were processed by removing interference signals (a standard process used for radio astronomy observations), Fourier analyzing the waveform data, and integrating the resulting spectrum over the basic pulse period of the transmissions. The analysis approach is basically similar to that used by the El Campo investigators.

5. Analysis of Selected Data

In Figure 4, we show the results of analysis of the experiment of 21 July 1996. On that day the interference level was relatively low, and the probability is high that the coronal return signal was detected. In the upper part of the figure, the transmitted pulse waveforms are shown, consisting of 20-sec period with 10-sec pulse width at full power. The waveform at 8.920 MHz is in opposite phase to the waveform at 8.880 MHz, so that full power was being transmitted at all times. In the 16-min interval, 48 transmission cycles occur. For the recorded signal from UT 0927 to 0943, the Fourier-analyzed data were integrated in 48 cycles to produce the integrated spectrum shown in the lower part of Figure 4. The vertical axes of the spectra correspond to the bandwidth of the receivers, with the transmitted frequency offset to the bottom side of each spectrum; thus, the measured frequency shifts are positive and correspond to Doppler shifts that would be caused by motion toward the earth. The horizontal axes correspond to the transmitted pulse periods. The color shading represents relative integrated power level; the dynamic range is about 1 dB with yellow being the high end and blue the low end of the scale. Thus, the color variation is indicative of variations in the signal-to-noise ratio. The red regions prominent at the tops of both spectra should be ignored, as these correspond to the roll-off the receiver filters. The regions of color-coding at the green and yellow level correpond to detected signals, and a comparison of the two spectra shows that, while the signal is weak, it has the expected phase relationship of the transmitted waveform. Thus, at a given frequency, the received signal-to-noise ratio is higher during the expected ON phase compared with the OFF phase. Also, comparing the two spectra shows that the ON phases are in opposition, as was the transmitted signal. Thus, the averaged spectra are consistent with a positive return from the solar corona. Because the dynamic range of the signal-to-noise ratio is low, on the order of 1 dB, we cannot attribute much signficance to apparent spectral details; it is possible that some features are remnants of interference signals or other noise sources. Therefore, we refer only to the total power comparisons and phase relationships of the spectra as an indication of positive detection. In Figure 5, we show the same data integrated in frequency to obtain a total relative

power comparison. The traces here show the relative power levels appear to be consistent with the transmitted waveform. Thus, we conclude from these observations that the return signal from the solar corona at about 9 MHz has been detected.

Other experiments that we have conducted generally produced less reliable results, due primarily to higher interference levels. Of the 8 experiments conducted in 1996, the data of 21 July were the best. We have continued these experiments in the summers of 1997 and 1998 also. During the 1997 experiments, we further investigated the use of several types of random coding for the transmissions, which can help to improve discrimination against background noise. Although we do not discuss it in this report, one of the 1997 experiments has also produced an apparent positive detection of a return signal. The data from the 1998 experiments have not been analyzed yet.

6. Summary and Conclusions

We have briefly reviewed the highlights of the early solar radar experiments at the El Campo facility and have described the characterisitics of the experiments and general results of analyses of radar echoes from the solar corona. The early solar radar experiments are a remarkable example of research that appears to have been ahead of its time. It is unfortunate that no comparable facility exists today that can benefit from the several correlative and detailed observations that are fairly routine in the modern era of space research. We have demonstrated that it is possible to use existing facilities for solar radar experiments by reporting a weak, but positive detection of the return signal in a recent experiment. It is also clear that with upgrades to current facilities, mainly for operation at higher frequency, significant solar radar capability can be recovered. New facilities, such as the HF Active Auroral Research Program (HAARP) radar, may allow several frequencies and diagnostics approaches to be used to detect CMEs. For example, the HAARP radar is steerable through the use of electronic phasing, and the final planned effective radiated power will be about 3 GW, which is greater than El Campo provided. Thus, with the more advanced state of understanding and experimentation of coronal physics at present, solar radar experimental research may be poised for a promising new beginning.

Acknowledgments. The work at the Naval Research Laboratory and at the SURA and UTR-2 facilities is supported by the Office of Naval Research and the Navy International Cooperative Opportunities in Science and Technology Program. We also acknowledge with gratitude the participation of Dr. Lev Erukhimov, and express our regret over his death in 1997.

Table 1. El Campo - SURA/UTR-2 System Comparison

The radar equation is

$$P_r = \frac{P_t G_t}{4\pi R^2} \frac{A_r \sigma p}{4\pi R^2}$$ where:

P_r - received power (watts)
P_t - transmitted power (watts)
G_t - transmitting antenna gain
A_r - receiving antenna area (m^2)
σ - scattering cross-section (m^2)
p - polarization fraction
R - range to scattering cross-section (m)
R_o - solar radius (m)

$R = 1.5 \times 10^{11}$ m (1 AU)
$R_o = 7 \times 10^8$ m (solar radius)
$\sigma \sim 1 \pi R_o^2 = 1.54 \times 10^{18}$ m^2 (typical value obtained by El Campo)
$p = 0.5$ (one of two polarizations)

$N = k_B T(f) B$ (noise power of sun), where

$k_B = 1.38 \times 10^{-23}$ watt-s $°K^{-1}$ (Boltzman's constant)
T(f) = noise equivalent temperature of sun (°K)
B = receiver bandwidth (Hz)

El Campo:

$P_t = 500$ kW
$G_t = 32$ dB
$A_{r1} = 18{,}000$ m^2 for one polarization
$A_{r2} = 9{,}000$ m^2 for cross polarization
$\sigma \sim 1 \pi R_o^2$
$P_r = 2.06 \times 10^{-16}$ watts

B = 50,000 Hz
$T(38 \text{ MHz}) = 8 \times 10^5$ °K
$N = 5.5 \times 10^{-13}$ watts
S/N = -34.0 dB

Ionospheric Loss ~ 1 dB
Signal processing (integration) gain: $\sim \sqrt{Bt}$, where
G ~ 38 dB

Net S/N ~ 3 dB

SURA/UTR-2:

$P_t = 750$ kW
$G_t = 19$ dB
$A_r = 150{,}000$ m^2 for one polarization

$\sigma \sim 1 \pi R_o^2$
$P_r = 8.23 \times 10^{-17}$ watts

B = 40,000 Hz
$T(9 \text{ MHz}) = 3 \times 10^5$ °K
$N = 1.7 \times 10^{-13}$ watts
S/N = -33.0 dB

Ionospheric Loss ~ 4 dB
t = 16 min = 960 s
G ~ 38 dB

Net S/N ~ 1 dB

Appendix

Solar Radar Investigators

P. Rodriguez
(Plasma Physics Division, Naval Research Laboratory, Washington DC)

A. Konovalenko, O. M. Ulyanov, S Stepkin, G. Inyutin, M. Sidorchuk, E. Abranin
(Radio Astronomy Department, Institute of Radio Astronomy, Kharkov, Ukraine)

L. Erukhimov, Y. I. Belov, Y. V. Tokarev, A. Karashtin, G. Komrakov
(Solar Terrestrial Physics Department, Radiophysical Research Institute, N Novgorod, Russia)

C. G .M. Vant Klooster
(ESTEC XEA, Noordwijk, The Netherlands)

SURA Radar Facility

SURA is located near Vasil'sursk, Russia and was built to conduct experiments in ionospheric modification by powerful radio waves, radar observations of the upper atmosphere and near earth space, and radio astronomy investigations. The radar array is composed of three sections, each section consisting of two sets of 48 crossed linear dipoles. Each set of crossed dipoles can be combined to give either right or left circular polarization when the array is operating. The overall array dimension is 300 x 300 meters. The array beam can be electronically steered over a declination range of 12° to 85° in 3° steps by manual and/or automatic phasing of the dipoles. Radar power is generated in three 250-kW transmitters that are connected independently to the three array sections. The three transmitters can also be operated in a coherent phase mode that results in an maximum effective radiated power of about 100 MW. In this mode, the beamwidth can be changed only in the N-S direction. A timing control system permits several regimes of operation of the transmitters, from minimum pulse widths of 50 milliseconds to continous wave (CW) transmission. The frequency stability is ensured by an internal frequency standard with the accuracy 10 E-7. External synchronization is also possible. Modulation modes include amplitude, phase, and combined amplitude-phase. The current operating frequency range is 4.6 to 9.3 MHz. The facility is currently undergoing an upgrade to allow transmission at higher frequencies, up 25 MHz.

The solar radar investigation is best done when the solar elevation is highest at SURA, or a zenith angle of 34° in July. In this case, the table below shows the system characteristics of one section of the SURA array with the antenna beam oriented toward the sun.

Sura Transmitting Array
Vasil'sursk, Russia

Operated by Radiophysical Research Institute
Nizhny Novgorod, Russia

Radiating elements: 144 crossed dipoles
Three subarrays: 90,000 m^2 total area
Three transmitters : 750 kW total (ERP~100 MW)
Frequency range = 4.6 - 9.3 MHz

Table A-1. SURA Transmission Characteristics

(Per 100 m x 300 m section radiating 250 kW at zenith angle 34°. For coherent phase combination of three sections, total effective radiated power ~ 100 MW.)

f (MHz)	Beam width (0.5 power)	Sun transit time* (min)	Antenna gain	Eff.Area (m^2)	Eff.Power/Section (MW)
9.31	6.1° x 22.1°	30	77 (±10%)	6400	19.2 (± 1dB)
9.05	6.3° x 22.8°	30	77 (±10%)	6700	19.2 (± 1dB)
8.90	6.3° x 22.8°	30	76 (±10%)	6875	19.2 (± 1dB)

* Observation time for bistatic (SURA/UTR-2) observations

UTR-2 Receiving Antenna Array

The UTR-2 antenna consists of two orthogonal multielement arrays of dipoles forming a T shape. The longest array is 1800 meters by 54 meters and is oriented along the local meridian. It consists of 1440 broadband horizontally polarized dipoles with axes in the east-west direction. The shorter north-south array is 900 meters long and 40 meters wide and consists of 600 horizontally polarized dipoles. The antenna currently operates between 8 and 32 MHz. At 9 MHz, the beam width in arc-minutes is 75' x 75', while at 25 MHz, the beamwidth is 27' x 27'. Depending on how the arrays are used, the effective collecting area varies from 50,000 to 150,000 m^2. The UTR-2 beam can be electronically scanned in right ascention and declination and can track the sun for 6 hours per day in summer. The minimum beam stepping time is 30 seconds. UTR-2 is routinely used to map out solar radio emissions and to investigate wave scattering and refraction effects from the corona. The high angular resolution permits the solar radar experiment to investigate possible return signals at scale sizes smaller than the early solar radar tests could provide. Because UTR-2 can provide continuous coverage of solar and ionospheric signal levels, the transmit/receive duty cycling of SURA does not reduce the overall probabilitity of detection of the return signal. Techniques used in radio astronomical studies to increase the signal-to-noise ratio of the received HF transmissions are used to process the data. The radio telescope is also designed to monitor sources of local interference in all frequency bands of operation. UTR-2 includes a system of absolute calibration with a standard noise generator and relative calibration with standard sky sources. At present, UTR-2 is the world's largest radio telescope in this frequency range. Further design details and operational modes of the UTR-2 radio telescope are discussed in Braude et al. [1978] and at this conference.

UTR-2 HF Receiving Array

Operated by Institute of Radio Astronomy
Kharkov, Ukraine

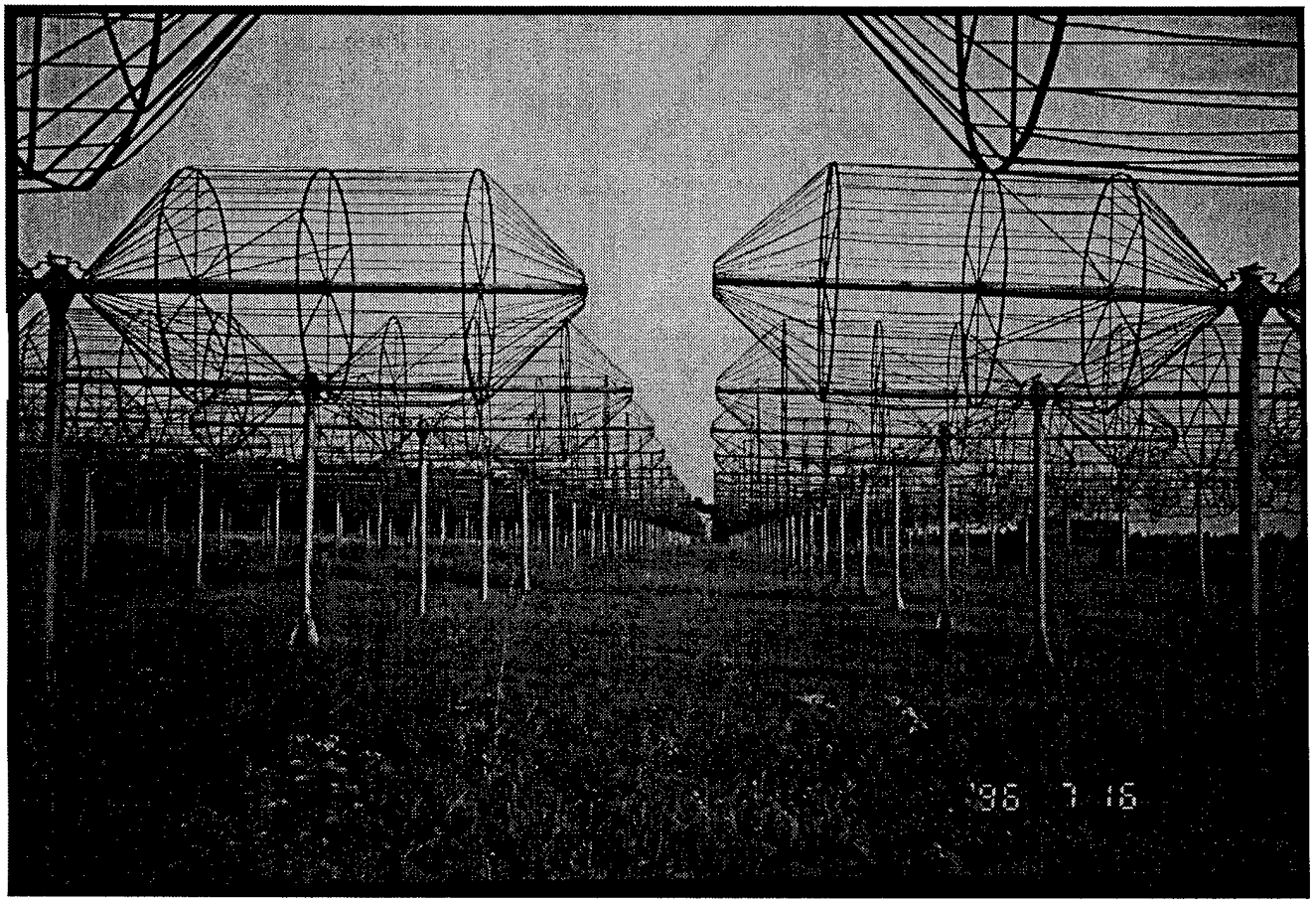

T-array:
1440 dipoles N-S
x 600 dipoles E-W
Total Area:
150,000 m^2
Sensitivity:
5 Jy @ 25 MHz
Frequency range:
8-32 MHz

High-speed digital registration

A six-channel tape recorder was used to record the signals from the UTR-2 North-South and East-West arrays. The bandwidth of each channel is 40 kHz. A high-speed A/D converter acquires the data for input to a computer. The output volume of data is approximately 2 or 3 Gigabytes for each experimental session. This system allows us to synthesize a pencil beam for the UTR-2 array. Rubidium standards are used for synchronization of all receivers and allow accurate measurements of the frequency of received signals, corresponding to a resolution of $\Delta f = 0.02$ to 0.05 Hz. A pilot signal is used with the tape recorder to compensate for tape speed wobble. This accuracy permits an estimate for scattering parameters at 9 MHz in the scattering medium.

Multichannel digital correlometer

The intermediate frequency signals with bandwidths up to 40 kHz from four radio receivers were input to four digital correlometers with 2 x 64 and 2 x 48 lags, obtaining a frequency resolution of about 1 kHz. One-bit digitization is used in the digital correlometers. This digitization leads to a decreased sensitivity by a factor of 1.57 but allows high reliability and stability of the receiver. Furthermore, this equipment allows us to reach a higher speed of sampling, with minimum memory requirement. The autocorrelation function is determined in real time with an integration constant of about 1 second. These data are input to a computer for storage and Fourier analysis. The maximum frequency coverage possible is about 100 kHz. As a maximum Doppler shift near 9 MHz, 100 kHz corresponds to a plasma flow velocity of 1500 km/sec. The nonlinear element at the input of the system increases the problem of intermodulation interference. During this project, the nonlinear problem was studied theoretically and experimentally. It was shown that, when the full power of the interference signal did not exceed the full power of the noise in the working frequency band, the interference is not significant. This situation existed during our experiments.

Video recorder

The video recorder was used to record the analog output of two radio receivers with bandwidths of 40 kHz. This facility includes mixers to transform intermediate band frequencies to baseband. The output of each receiver is split into In-phase and Quadrature channels. The number of quantization levels is four. The signals are sent by computer in digital form to a video recorder. Furthermore, precise time signals are recorded on the video recorders. Data processing begins in the off-line regime with tape playback to a computer, followed by spectrum analysis and determination of various parameters of the recorded signal.

Multichannel postdetection recording

Thirty radio receivers are used in the frequency range from 8 to 32 MHz for the 5-beam mode of the UTR-2 array. The signals from the outputs of the detectors and integrators are digitized. The minimum sampling period is near 2 millisec. This facility is used to obtain reference reflection signals from the moon and to monitor standard radio sources; these sources provide a method of monitoring the effects of ionospheric influence on the received signals. The level of received signals is not known a priori because the amplification of each channel is different. In order to reduce ionospheric refraction effects, the received signals are distributed along spatially separated beams. For the observation of reference radio sources, the frequency band is 4 kHz to 40 kHz, with time constants of 1 sec to 60 sec.

Sporadic solar radio emissions

A 9- to 30-MHz multichannel receiving system with high dynamic range is used as a background solar monitor. The time resolution is near 100 milliseconds. Usually, the observations are carried out in eight channels with bandwidths approximately 10 kHz near the frequencies of 8.9, 10, 12.6, 14.7, 16.7, 20, 25, and 30 MHz. Furthermore, it is possible to use a broadband dynamic spectrograph and heliograph for spatial localization of emission sources. This system allows us to record sporadic radio emission and corresponding dynamic spectra.

WIND/WAVES HF Receiver

The WAVES experiments on the WIND spacecraft provides a stepped frequency receiver with 256 frequency channels from 1.075 MHz to 13.825 MHz, in 50-kHz intervals, with 20 kHz bandwidth. The cycle time of the receiver is 16.192 sec, with the effective dwell time per frequency being 60 ms. This receiver can be programmed to step through all frequency channels or to continuously sample only one channel. Special modes to alternately sample two channels corresponding to SURA transmissions have been designed for this investigation. The detection is done with a spin axis dipole of 11-meter length with a detection threshold of ~7 nvolt/$\sqrt{\text{Hz}}$. A second spin plane dipole of 15-meter length rotates with the spacecraft at a 3-sec period. The orbit of WIND covers radial distances from 10 Re to 250 Re, where Re is in earth radii. Transmissions from SURA (and HAARP) have been received by the WAVES experiment at all WIND radial distances.

References

Abel, W. G., J. H. Chisholm, P. L. Fleck, and J. C. James, Radar reflections from the sun at very high frequencies, *J. Geophys. Res.*, **66**, 4303, 1961.

Abel, W. G., J. H. Chisholm, and J. C. James, Radar reflections from the sun at VHF, in *Space Res. III*, edited by W. Priester, North Holland Publishers, Amsterdam, p 635-643, 1963.

Allen, C. W., *Astrophysical Quantities*, 3rd ed., the Athlone Press, Univ. of London, 1973.

Bass, F. G., and S. Ya. Braude, On the question of reflecting radar signals from the sun, *Ukr. J. Phys.*, **2**, 149, 1957.

Braude, S. Ya., A.V.Megn, B.P.Ryabov, N.K.Sharykin and I.N.Zhouck Decametric survey of discrete sources in the northern sky, *Astrophys. Space Sci.*, **54**, 3, 1978.

Chashei, I. V., and V. I. Shishov, Volume scattering model for interpretation of solar radar experiments, *Solar Phys.*, **149**, 413-416, 1994.

Crooker, N., J. A. Joselyn, and J. Feynman, editors, *Coronal Mass Ejections*, Geophysical Monograph **99**, American Geophysical Union, 1997.

Eshleman, V. R., R. C. Barthle, and P. B. Gallagher, Radar echoes from the sun, *Science*, **131**, 329-332, 1960.

Genkin, L. G., and L. M. Erukhimov, Interplanetary plasma irregularities and ion acoustic turbulence, *Phys. Repts.*, **186**, 97, 1990.

Genkin, L.G., L.M.Erukhimov, and Yu.V.Tokarev. Diagnostics of ion-acoustic turbulence in the solar wind by the method of radio wave scattering. *Proc. of the III URSI Symp. on Modification of the Ionosphere by Powerful Radio Waves(ISIM-3)*, Suzdal, USSR, Sept.9-13, 171, 1991.

Gerasimova, N. N., Comparison of results of radar studies of the corona with solar activity, *Sov. Astron.*, **18**, 482, 1975.

Gerasimova, N. N., Efficiency of four-plasmon interactions in the reflection of a radar signal from the sun, *Sov. Astron.*, **23**, 738, 1979.

Gordon, I. M., Interpretation of radio echos from the sun, *Astrophys. Lett.*, **2**, 49, 1968.

Gordon, I. M., Radar exploration of the sun and physical processes of the solar corona, *Astrophys. Lett.*, **3**, 181, 1969.

Gordon, I, M., Plasma theory of radio echoes from the sun and its implications for the problem of the solar wind, *Space Sci. Rev.*, **15**, 157, 1973.

Gurevich A. V., A. N. Karashtin, A. M. Babichenko, I. N. Kazarov, and G. P. Komrakov, HF magnetosphere sounding at SURA, *Proc. 21st Remote Sensing Society Ann. Conf.*, Southampton, UK, p. 1333-1340, 1995.

James, J. C., Radar studies of the sun, in *Radar Astronomy*, edited by J. V. Evans and T. Hagfors, McGraw Hill Book Company, New York, 1968.

James, J. C., Some observed characteristics of solar radar echoes and their implications, *Solar Phys.*, **12**, 143-162, 1970a.

James, J. C., Some characteristics of the solar atmosphere that may be investigated by a VHF antenna system, *JPL Technical Report* **32-1475**, 1970b.

Kerr, F. J., On the possibility of obtaining radar echoes from the sun and planets, *Proc. IRE*, **40**, 660, 1952.

Mel'nik, V. N., Plasma theory of solar radar echoes, poster at this Chapman Conference, 1998.

Owocki, S. P., G. A. Newkirk, and D. G. Sime, Radar studies of the non-spherically symmetric solar corona, *Solar Phys.*, **78**, 317-331, 1982.

Pottasch, S. R., Use of the equation of hydrostatic equilibrium in determining the temperature distribution in the outer solar atmosphere, *Astrophys. J.*, **131**, 68-74, 1960.

Rodriguez, P., High frequency radar detection of coronal mass ejections, *Proceedings of the 16th NSO/Sacramento Peak International Workshop on Solar Drivers of Interplanetary and Terrestrial Disturbances*, ASP Conference Series, Vol. **95**, 180-188, 1996.

Rodriguez, P., E. J. Kennedy, M. J. Keskinen, C. L. Siefring, Sa. Basu, M. McCarrick, J. Preston, M. Engebretson, M. L. Kaiser, M. D. Desch, K. Goetz, J.-L. Bougeret, and R. Manning, The WIND-HAARP experiment: initial results of high power radiowave interactions with space plasmas, *Geophys. Res. Lett.*, **25**, 257, 1998.

van't Klooster, C.G.M., Yu. Tokarev, Yu. Belov, A. A. Konovalenko, and P. Rodriguez, Transmission of high power 9 MHz signals near ionospheric cut-off from 'Sura' towards the moon and reception of the echo with the radio telescope 'UTR2', in *10th International Conference on Antennas and Propagation*, Conference Publication No. 436, 2.35, 1997.

Wentzel, D. G., A new interpretation of James's solar radar echoes involving lower-hybrid waves, *Astrophys. J.*, **248**, 1132-1143, 1981.

Figure Captions

Figure 1. Aerial view of El Campo solar radar array. The long axis is in the north-south direction, thus providing a fan beam in the east-west direction. Characteristics of the array are listed.

Figure 2a. Composite of range-amplitude measurements from several publications of the El Campo results. As the transmitted pulse width was reduced from 8 s to 1 s, the corresponding range resolution increased, and the total range decreased. The plots are scaled to keep the solar diameter approximately the same.

Figure 2b. The typical El Campo range-doppler-amplitude spectra for pulse widths $\leq$ 1 s. The size of the black shading in each range-doppler cell is proportional to the integrated signal/noise ratio of the solar echo. The range scale is adjusted according to the coronal density model used. For the spectrum shown the maximum echo signal is observed between 1 and 1.5 Ro.

Figure 3. Schematic of the concept for detecting coronal mass ejections with an HF solar radar. A bistatic arrangement is shown, with the transmitting site separated from the receiving site. In the lower right-hand corner, a schematic of the echo signal frequency spectrum is shown. The transmitted signal at a given frequency is shown along with the expected echo spectra. A "normal quiescent" corona may produce a broad range of frequency shifts, while a CME event may produce a more distinct doppler shift.

Figure 4. The data from the Sura/UTR-2 experiment of 21 July 1996. The upper panel shows the pulse pattern transmitted by Sura in the 16-min interval between UT 0911 and 0927 at two frequencies separated by 40 kHz. The lower panels show the dynamic spectra of the echo signals received during the 16-min interval between UT 0927 and 0943. The spectra are integrated over 20-s sub-intervals corresponding to the transmitted 20-s pulse period.The receiver frequency is shown on the frequency axis of each spectrum. The receiver bandwidth (44 kHz) determines the frequency range of each spectrum. The color coding covers a range of about 1 dB in signal to noise ratio. Above about 35 kHz the receiver filter roll-off determines the spectra color coding and should be ignored. The yellow and green colors correspond to the echo during the ON and OFF phases of the transmitted signal. A careful comparison of the total powers in the ON phases with the OFF phases illustrates that the echo intensities have the same phase relationship as the transmitted signals, providing high probability that a true echo signal is detected. However, no clear evidence of an echo from a CME is evident; the spectra appear to correspond to an echo from a normal corona.

Figure 5. The data of Figure 4 displayed in two-dimensional integrated form. The upper panel is the time profile of the 16-min integrated echo signal at the two receiver frequencies. The pulse patttern is shown for comparison and shows that the integrated echo signal shows a similar phase relationship. The lower panel shows the 16-min integrated frequency spectra of the 44-kHz receiver bandwidth. No well-defined frequency "peaks" correponding to a doppler shift from a CME are evident; thus, only a quiescent coronal echo is suggested.

Solar Radar Antenna
El Campo, Texas

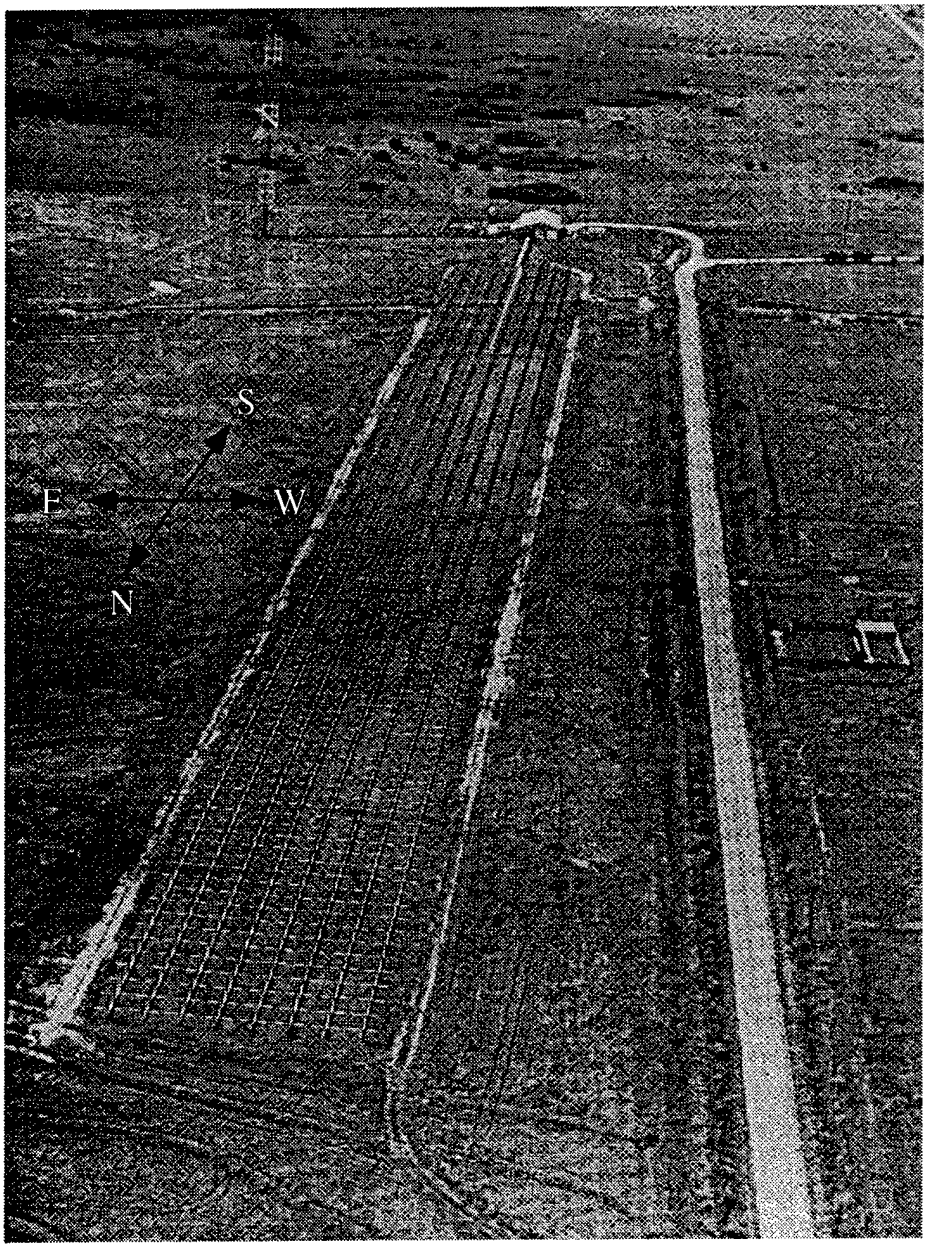

Transmitting $\lambda/2$ dipoles: 128 x 8 EW

Receiving $\lambda/2$ dipoles: 128 x 8 EW, 128 x 4 NS

Total Area: 18,000 m^2 Power: 500 kW

Antenna Gain: 32-36 dB ERP: 1300 MW

Frequency: 38.25 MHz BW: 1° x 6 ° NS x EW

Figure 1

El Campo Solar Radar Measurements

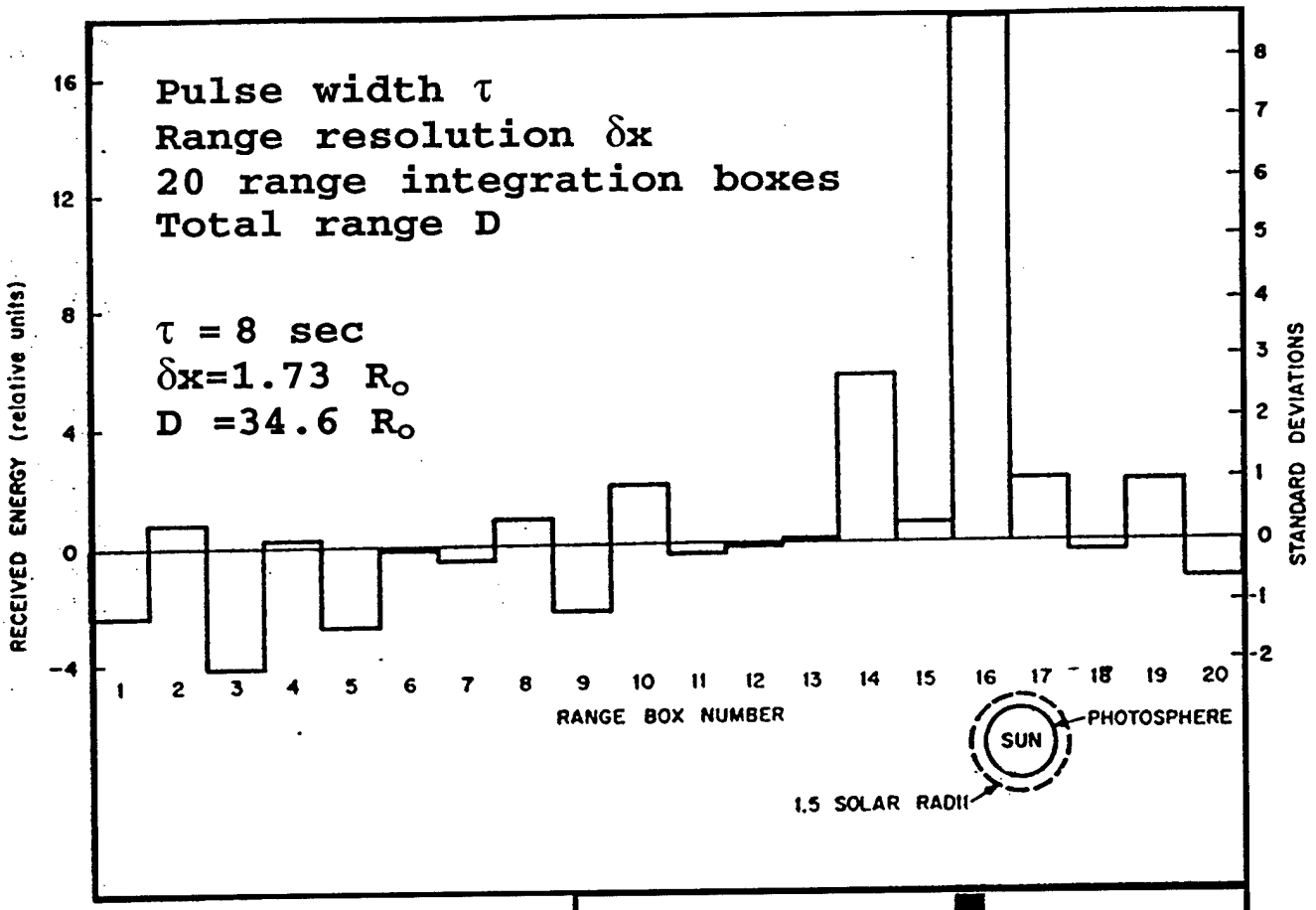

τ = 4 sec
δx=0.86 R₀
D =17.2 R₀

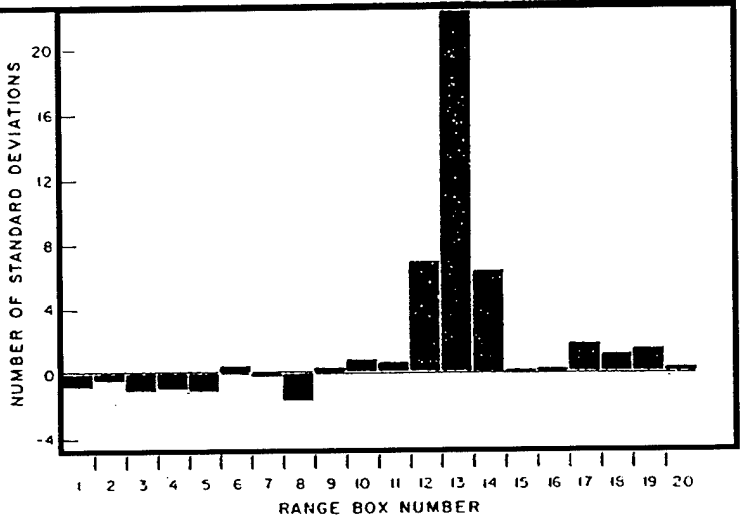

τ = 2 sec
δx=0.43 R₀
D = 8.6 R₀

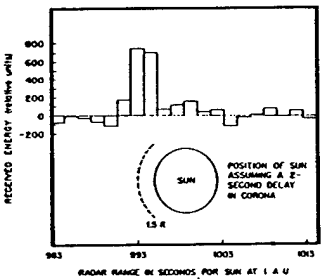

τ = 1 sec
δx=0.22 R₀
D = 4.4 R₀

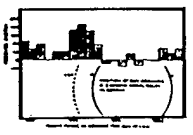

Figure 2a.

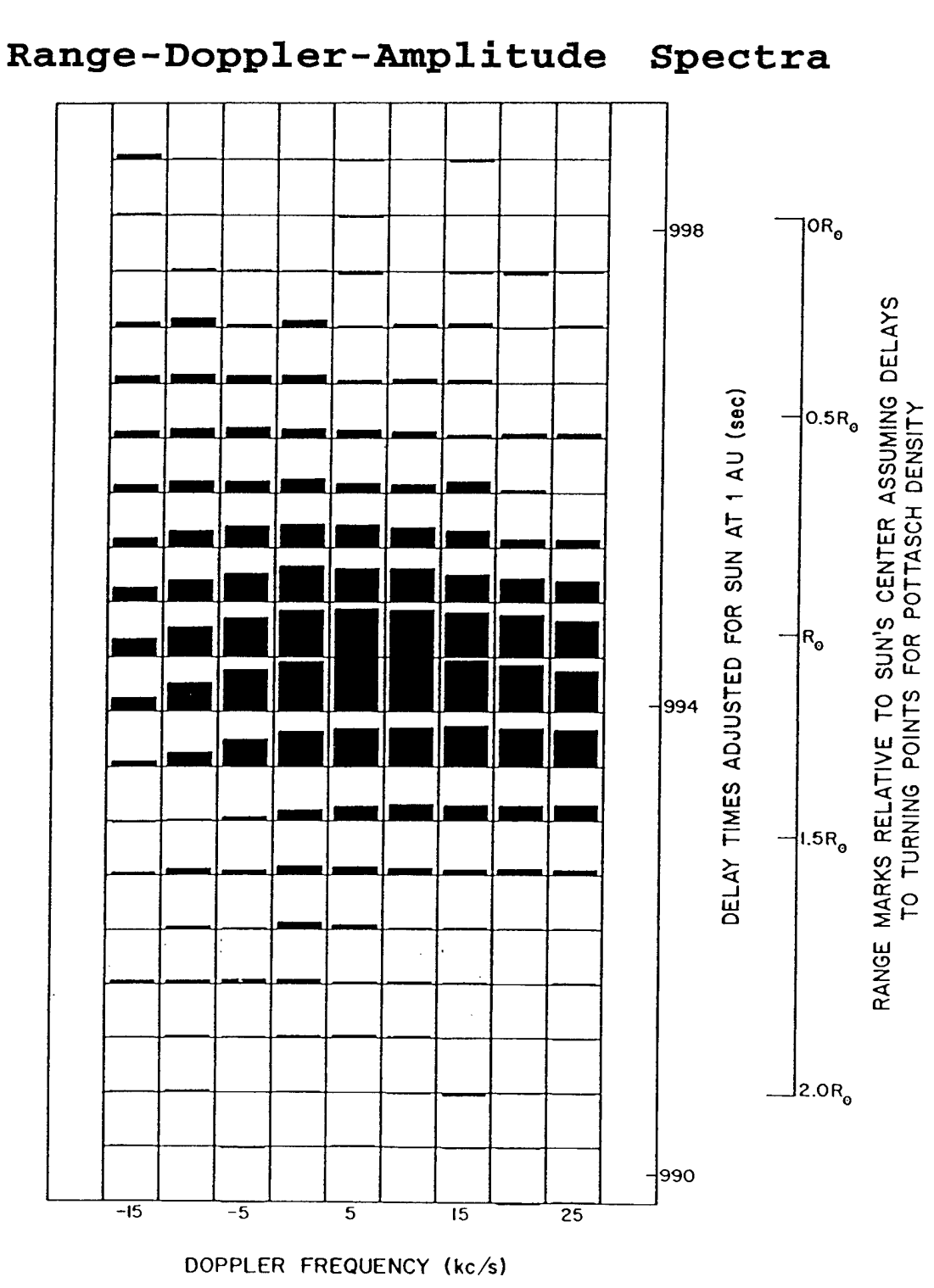
El Campo Solar Radar
Range-Doppler-Amplitude Spectra
998
994
990
-15
-5
5
15
25
DOPPLER FREQUENCY (kc/s)
DELAY TIMES ADJUSTED FOR SUN AT 1 AU (sec)
0R⊙
0.5R⊙
R⊙
1.5R⊙
2.0R⊙
RANGE MARKS RELATIVE TO SUN'S CENTER ASSUMING DELAYS
TO TURNING POINTS FOR POTTASCH DENSITY

Figure 2b.

Solar Radar Detection of Earthward-Directed Coronal Mass Ejections

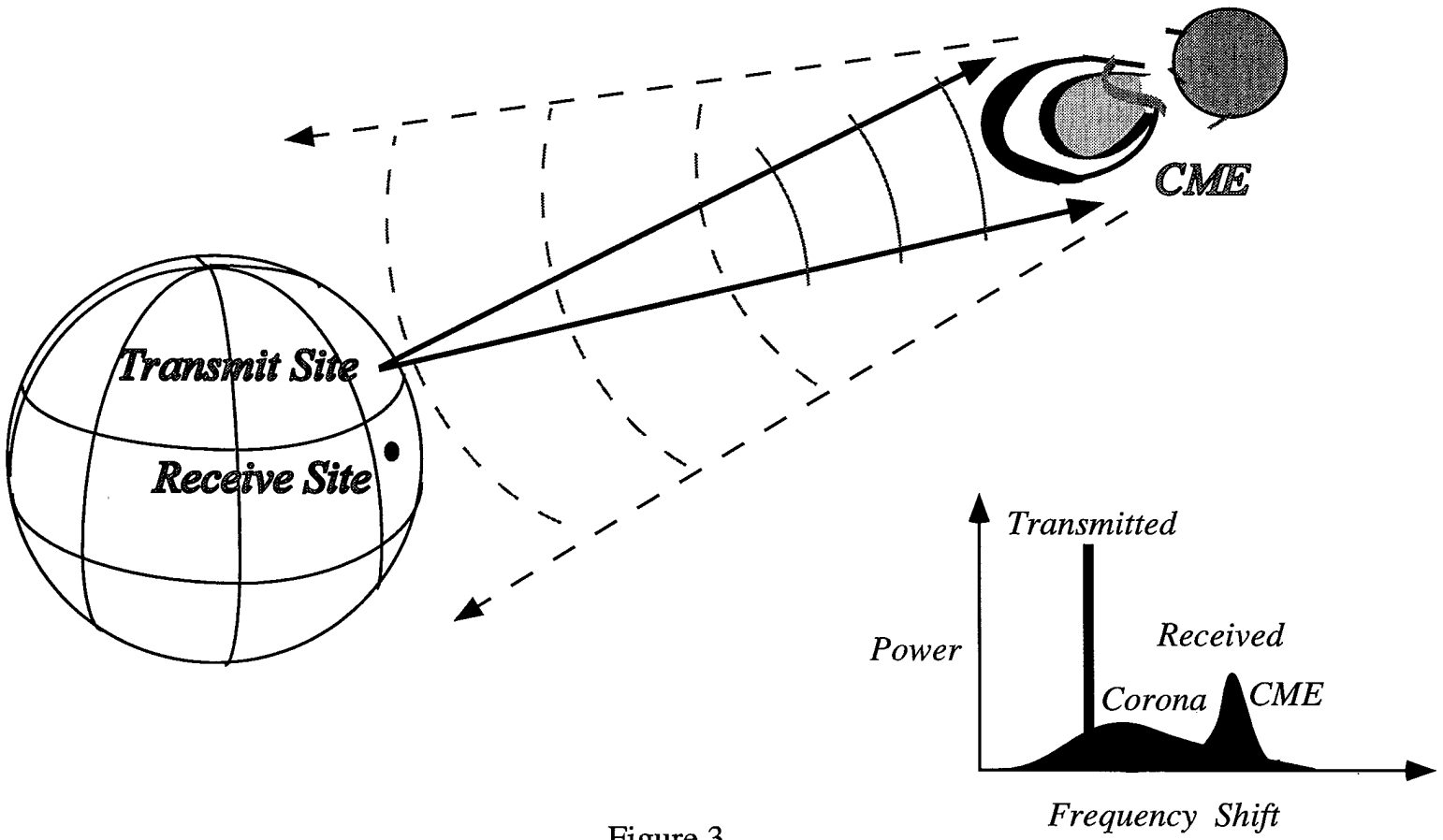

Figure 3

Solar Radar Experiment 21 July 1996

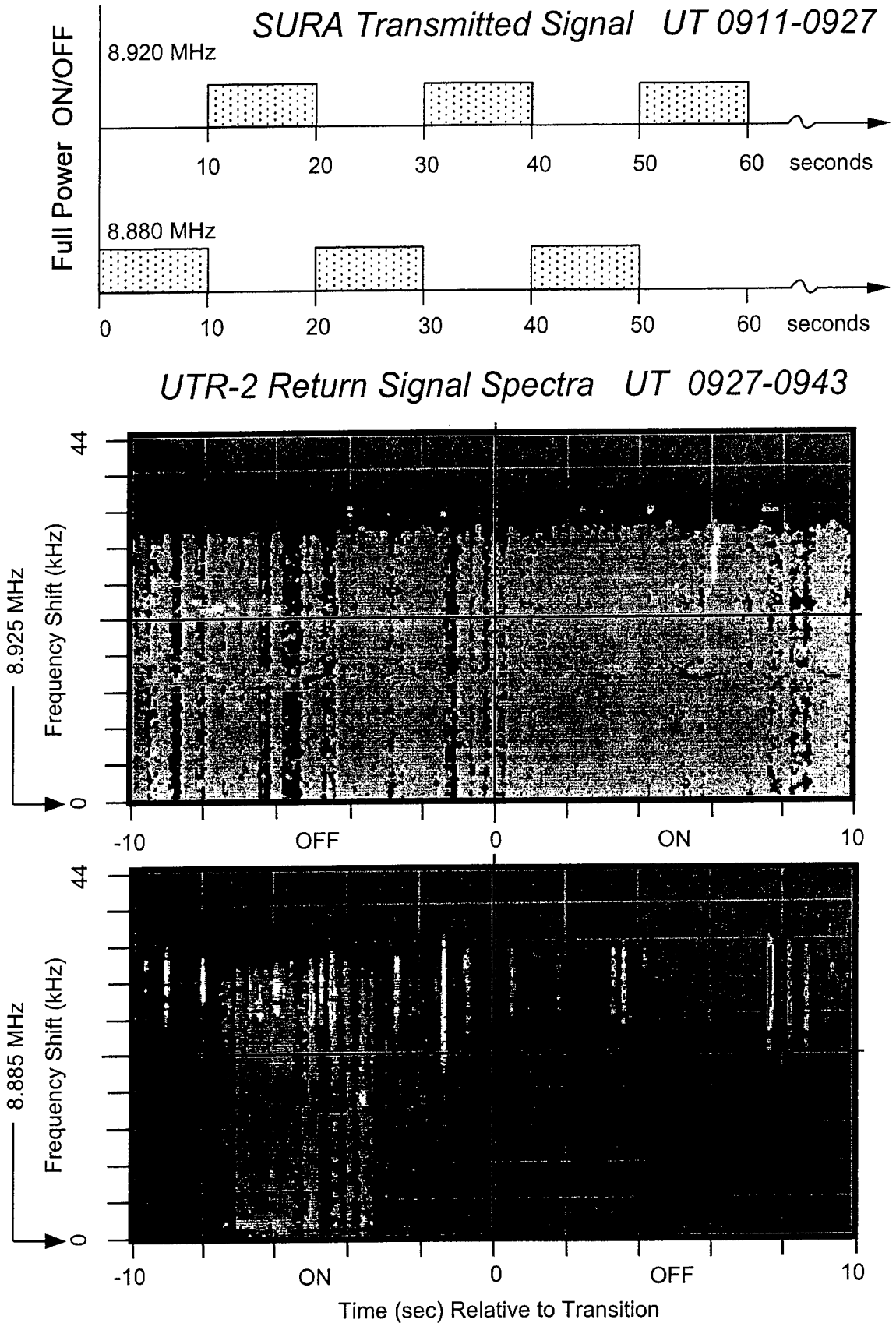

Figure 4

Integrated Return Signal Time Profiles and Spectra

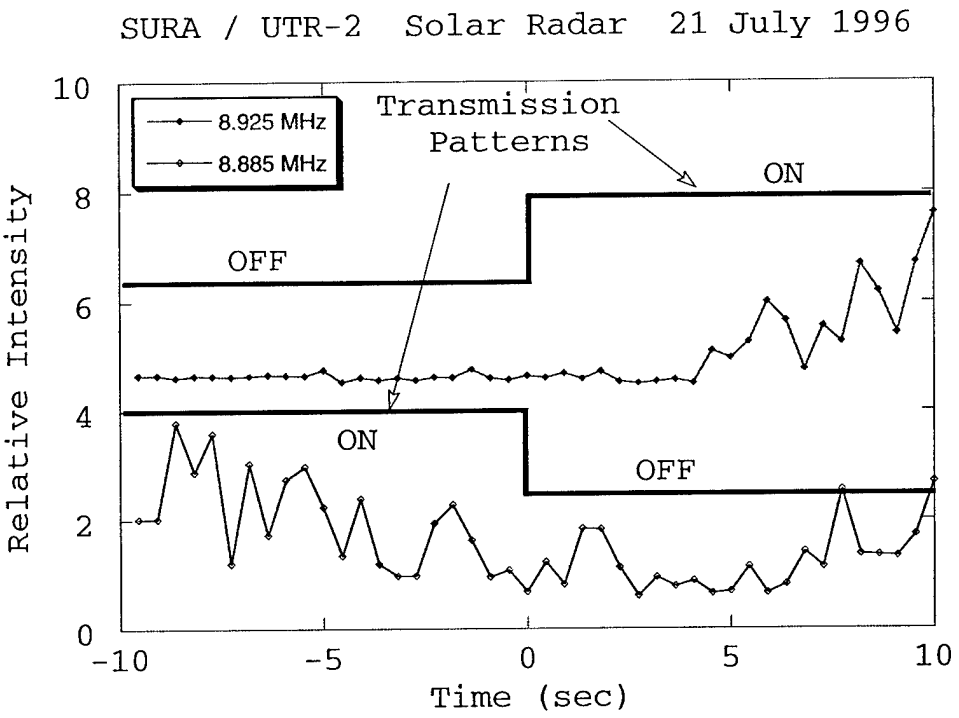

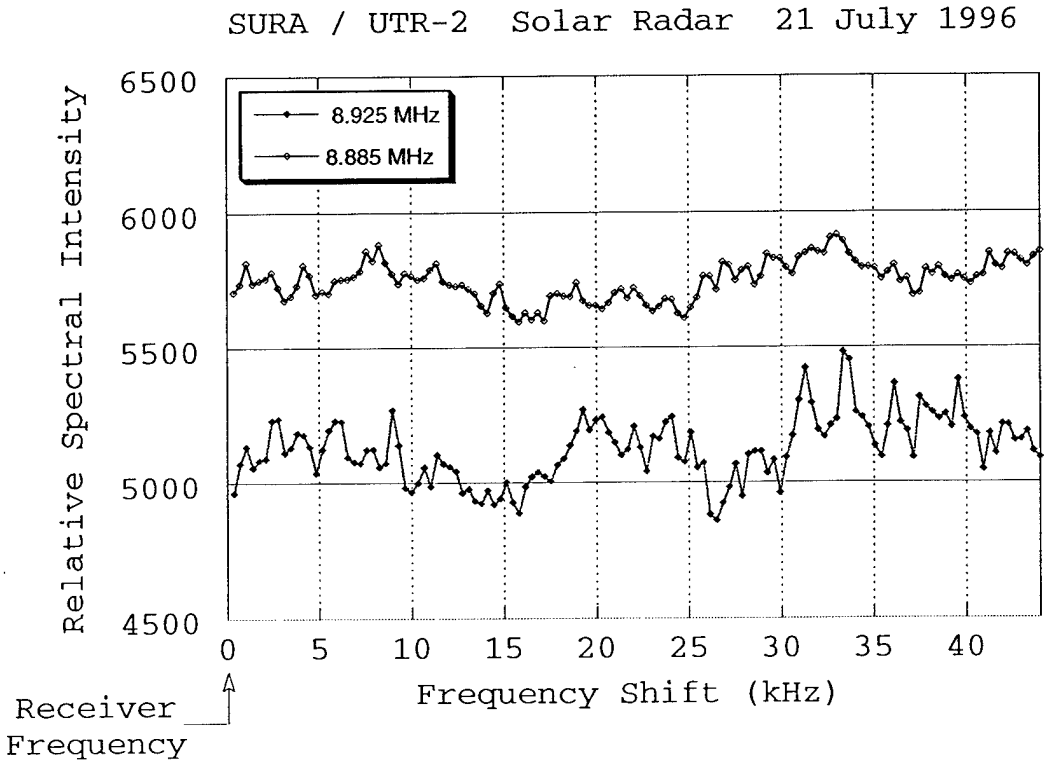

Figure 5